# Structural determination of wild-type lactose permease

Lan Guan*, Osman Mirza[†‡], Gillian Verner*, So Iwata[‡§¶], and H. Ronald Kaback*[‖]

*Department of Physiology and Department of Microbiology, Immunology, and Molecular Genetics, Molecular Biology Institute, University of California, Los Angeles, CA 90095-1662; [†]Department of Medicinal Chemistry, Faculty of Pharmaceutical Sciences, University of Copenhagen, Universitetsparken 2, 2100 Copenhagen, Denmark; [‡]Division of Molecular Biosciences, Imperial College London, London SW7 2AZ, United Kingdom; [§]Exploratory Research for Advanced Technology Human Receptor Crystallography Project, Kawasaki, 210-0855 Kanagawa, Japan; and [¶]RIKEN Genomics Sciences Center, 1-7-22 Suchiro-cho, Tsumi, Yokohama 230-0045, Japan

Contributed by H. Ronald Kaback, August 15, 2007 (sent for review August 3, 2007)

**Here we describe an x-ray structure of wild-type lactose permease (LacY) from *Escherichia coli* determined by manipulating phospholipid content during crystallization. The structure exhibits the same global fold as the previous x-ray structures of a mutant that binds sugar but cannot catalyze translocation across the membrane. LacY is organized into two six-helix bundles with twofold pseudosymmetry separated by a large interior hydrophilic cavity open only to the cytoplasmic side and containing the side chains important for sugar and $H^+$ binding. To initiate transport, binding of sugar and/or an $H^+$ electrochemical gradient increases the probability of opening on the periplasmic side. Because the inward-facing conformation represents the lowest free-energy state, the rate-limiting step for transport may be the conformational change leading to the outward-facing conformation.**

conformation | mechanism | membrane protein | transport | x-ray structure

Lactose permease (LacY) belongs to the major facilitator superfamily (www.tcdb.org), a very large group of membrane transport proteins that are evolutionarily related. LacY carries out the coupled stoichiometric symport of a galactoside with an $H^+$, using the free energy released from downhill translocation of $H^+$ to drive accumulation of galactosides against a concentration gradient (see ref. 1). Notably, in the absence of an electrochemical proton gradient [interior negative and/or alkaline ($\Delta\bar{\mu}_{H^+}$)], LacY also catalyzes the converse reaction, using free energy released from downhill translocation of sugar to drive uphill translocation of $H^+$ with generation of $\Delta\bar{\mu}_{H^+}$, the polarity of which depends on the direction of the substrate concentration gradient. LacY also catalyzes exchange or counterflow of sugar without translocation of $H^+$, and these reactions are unaffected by $\Delta\bar{\mu}_{H^+}$. Therefore, it is likely that the primary driving force for turnover is binding and dissociation of sugar on either side of the membrane.

The previous x-ray structures of LacY (2, 3) were obtained from the conformationally constrained C154G mutant (4, 5). The structures provide critical information regarding the overall fold and confirm for the most part the position of residues involved in sugar binding and $H^+$ translocation. Site-directed biochemical, biophysical, and immunological techniques in conjunction with functional studies and the crystal structures have led to a working model for lactose/$H^+$ symport where the sugar-binding site is alternatively open to either side of the membrane (1, 2, 6, 7, 44). Notably, an alternating access model has also been proposed for GlpT (8) and the ATP-binding cassette transporters (9, 10), suggesting a common global conformational change for solute transport across the membrane.

The C154G mutant is severely crippled with respect to sugar translocation (4, 11), although the mutant binds ligand as well as the wild type [ref. 5; supporting information (SI) Fig. 4 and *SI Text*]. It is essential to obtain a crystal structure for wild-type LacY, but crystallization attempts for well over a decade failed. By adjusting phospholipid (PL) content during crystallization, wild-type LacY was finally crystallized in a form that diffracts to a resolution similar to the C154G mutant (2, 12). The structure of wild-type LacY is presented here.

## Results

**Global Fold.** An x-ray crystal structure of wild-type LacY was solved to a resolution of 3.6 Å (Fig. 1*A*). The protein was cocrystallized in the presence of 5 mM β-D-galactopyranosyl 1-thio-β-D-galactopyranoside (TDG). Data collection and refinement statistics are summarized in Table 1. The overall fold and helix packing of wild-type LacY are indistinguishable from the structure of the C154G mutant, with rmsd values for the Cα atoms of 1.2 Å for the ligand-bound [1pv7 (2)] and 1.5 Å for the unbound C154G [2cfp (3)] structures, respectively. LacY is organized as two six-helix bundles connected by a long loop between helices VI and VII. The N- and C-terminal six-helix bundles exhibit twofold pseudosymmetry. Similar to other members of the major facilitator superfamily, GlpT (8) and EmrD (13), additional twofold pseudosymmetry is observed within each domain, indicating that the N- and C-terminal domains have the same genetic origin (14).

A large hydrophilic cavity is open only to the cytoplasmic side with greatest dimensions of 25 × 15 Å (Fig. 1*B*). The hydrophilic cavity is lined with helices I, II, IV, and V in the N-terminal domain and helices VII, VIII, X, and XI in the C-terminal domain. Helices III, VI, IX, and XII are largely embedded in the bilayer, as suggested (6, 15). Many of the helices, particularly those forming the internal cavity, are very distorted (Fig. 1 *B* and *C*). The distorted helices, large hydrophilic cavity, and conformational flexibility provide an explanation for the very high rate of backbone H/D exchange observed with LacY (16, 17). Moreover, the periplasmic ends of helices I (Pro-28, Pro-31, Ile-32, His-35) and VII (Gln-241, Gln-242, Ala-244, Asn-245, and Thr-248) form a gateway to the binding site (Fig. 1*A*) with Ile-32 and Asn-245 sealing the cavity from the periplasm (Fig. 1 *B* and *C*).

**Sugar-Binding Site.** The native structure of wild-type LacY was cocrystallized with 5 mM TDG. No clear density for the sugar was observed within the hydrophilic cavity; however, all residues essential for sugar binding showed clear electron densities (Fig. 2*A*), and their positions were determined unambiguously. The

Author contributions: L.G. and H.R.K. designed research; L.G. and G.V. performed research; and L.G., O.M., S.I., and H.R.K. analyzed data and wrote the paper.

The authors declare no conflict of interest.

Abbreviations: LacY, lactose permease; DDM, dodecyl β-D-maltopyranoside; PL, phospholipids; TDG, β-D-galactopyranosyl 1-thio-β-D-galactopyranoside; $\Delta\bar{\mu}_{H^+}$, electrochemical proton gradient (interior negative and/or alkaline).

Data deposition: The coordinates and structure factors have been deposited in the Protein Data Bank, www.pdb.org (PDB ID code 2v8n).

[‖]To whom correspondence should be addressed. E-mail: rkaback@mednet.ucla.edu.

This article contains supporting information online at www.pnas.org/cgi/content/full/0707688104/DC1.

© 2007 by The National Academy of Sciences of the USA

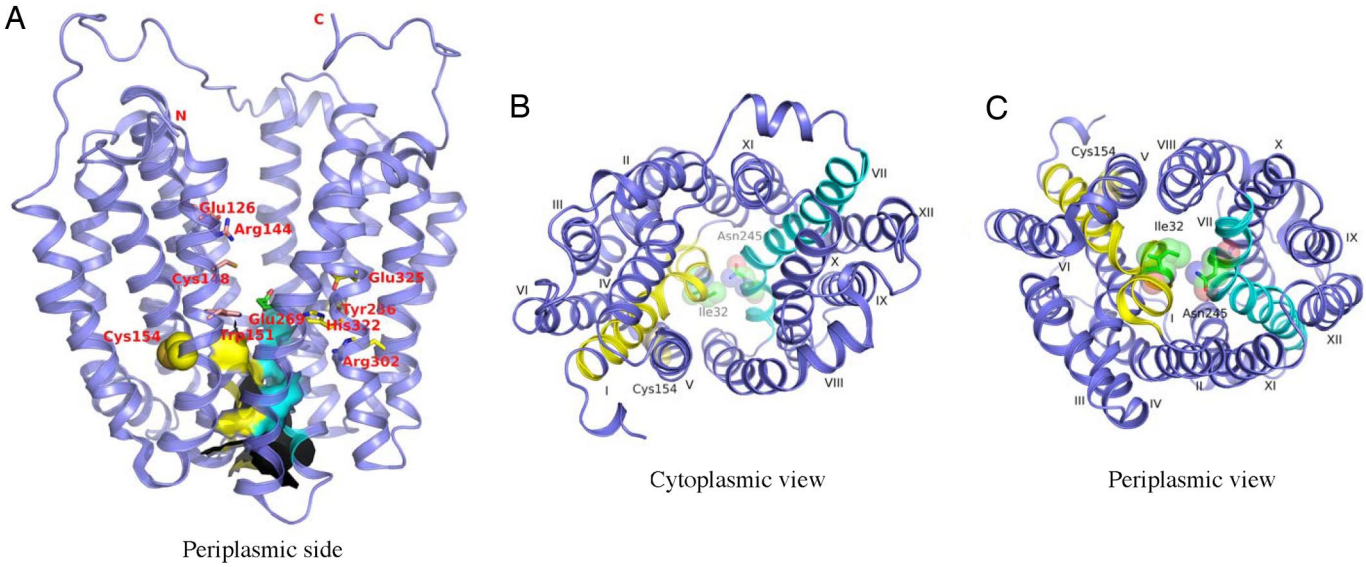


**Fig. 1.** Cartoon representation of the overall structure of wild-type LacY. (*A*) The residues involved in substrate binding [Glu-126 (helix IV), Arg-144, Cys-148, and Trp-151 (helix V)] are shown as pink sticks, and those involved in $H^+$ translocation [Tyr-236 (helix VII), Arg-302 (helix IX), His-322, and Glu-325 (helix X)] are shown in yellow. The dual-function residue Glu-269 (helix VIII) is shown in green. Cys-154 is shown as van der Waals spheres (yellow). Pro-28, Pro-31, Ile-32, and His-35 on helix I (yellow surface) and Gln-241, Gln-242, Ala-244, Asn-245, and Thr-248 on helix VII (cyan surface) form a periplasmic gateway. The black color represents the back side of the surfaces. (*B*) View from cytoplasmic side with Ile-32 (helix I) close to Asn-245 (helix VII) shown as sticks with transparent van der Waals spheres (green). (*C*) View from periplasmic side with Ile-32 close to Asn-245.

configuration of these residues [Glu-126 (helix IV), Arg-144, Trp-151 (helix V), and Glu-269 (helix VIII)] (Fig. 2*B*; gray) is similar to that observed in C154G LacY without ligand (Fig. 2*B*, pink; 2cfp) (3). Arg-144 is within salt-bridge distance from Glu-126 (18–20), and Glu-269 is in close proximity to Trp-151 (21, 22) (Fig. 2*B*).

Although Cys-148 (helix V) is not irreplaceable, many studies suggest that this side chain may interact with the hydrophobic face of galactopyranosides and galactose (23–27). Previous structures of C154G LacY (2, 3) were solved with crystals grown from protein modified with methyl mercury acetate. Therefore, it is not surprising that the side chain of Cys-148 is far from the sugar-binding site in the previous structures. In the native structure of wild-type LacY, the sulfur atom of Cys-148 is moved 2.7 Å toward the sugar-binding site and is positioned between essential residues Arg-144/Glu-269 and the aromatic residue Trp-151 (28) (Fig. 2 *A* and *B*).

The residues that are likely involved directly in $H^+$ translocation, which include Glu-269 (helix VIII), His-322 and Glu-325 (helix X), Arg-302 (helix IX), and Tyr-236 (helix VII) (1, 29), are exposed to the same cavity and located at a similar level as the sugar-binding site in the membrane (Fig. 1*A*).

**Cys-154.** The $F_o - F_c$ electron density of the side chain of Cys-154 (helix V) is shown in Fig. 3*A*. Cys-154 is located in a unique position, just below three residues directly involved in sugar binding (Arg-144, Cys-148, and Trp-151), just above the periplasmic gateway (Fig. 1*A*). The sulfur atom of Cys-154 forms two H bonds with the carbonyl oxygens of Phe-21 and Gly-24 (helix I), respectively (Fig. 3*B*). In contrast to the wild type, an empty space is observed where Cys-154 is replaced with Gly (2, 3), suggesting less intimate contact between helices I and V in this conformation of the mutant.

## Discussion

It is well known that the intrinsic hydrophobic properties of membrane proteins represent a bottleneck to crystallization. Purified membrane proteins are protein–detergent–PL complexes that are difficult to reproduce and maintain in a homogeneous state. The importance of PL in crystallization of membrane proteins has been described (30–35). In C154G LacY, three different crystal forms diffract to increasingly better resolution in a manner that correlates with the concentration of copurified PL (2, 3, 12). In the crystallization of wild-type LacY, a big problem is batch-to-batch variation. To a great extent, this may be due to loss of bound PL during purification. Accordingly, replenishment of PL is critical for crystallization of LacY (12), and optimization of the ratio of PL–detergent–precipitant (polyethylene glycol) for each protein preparation with purified *Escherichia coli* PL improves the reproduction of high-quality crystals for structure determination.

The apo structure of wild-type LacY exhibits an inward-facing conformation. Notably, all four available structures of the C154G mutant solved from two different crystal forms have the same global fold (2, 3). Furthermore, in right-side-out membrane vesicles, several single-Cys mutants in the periplasmic gateway to the sugar-binding site react poorly with alkylating agents unless a liganding sugar is presented (6, 45), indicating that in the absence of sugar, the periplasmic barrier is tightly closed. Therefore, the inward-facing conformation of LacY probably represents the lowest free-energy state in detergent solution and in the membrane.

Previous studies (36) show that the reactivity of single-Cys-122 LacY with the affinity inactivator methanethiosulfonyl galactoside, but not the glucoside homologue, increases fifty-fold in the presence of $\Delta\bar{\mu}_{H^+}$ (interior negative), which is observed exclusively with right-side-out and not with inside-out vesicles. Although $\Delta\bar{\mu}_{H^+}$ exhibits no effect on binding affinity from either side of the membrane (37), it enhances the reactivity of several of the same single-Cys mutants in the periplasmic gateway that exhibit TDG-induced increases in reactivity with thiol reagents (45). The observations indicate that sugar on the periplasmic side of the membrane or $\Delta\bar{\mu}_{H^+}$ (interior negative) leads to formation of a hydrophilic pathway that allows access to the sugar-binding site (6). These observations support the idea that sugar and/or $\Delta\bar{\mu}_{H^+}$ alter conformational equilibria by increasing the probability of the out-

**Table 1. Data collection and refinement statistics**

| | |
|---|---|
| Data collection (ALS BL8.2.1) | |
| Wavelength, Å | 1.000 |
| Resolution, Å | 40.0–3.6 (3.73–3.6) |
| Total reflections | 54,155 |
| Unique reflections | 24,578 |
| Redundancy | 2.5 |
| Completeness, %* | 85.8 (75.6) |
| $R_{sym}$, %*† | 0.12 (0.49)‡ |
| Refinement | |
| Resolution, Å* | 10.0–3.6 (3.81–3.6) |
| $R$ factor, %*§ | 29.4 (39.2) |
| $R_{free}$, %*¶ | 33.3 (41.6) |
| rms deviations from ideal values | |
| Bond lengths, Å | 0.011 |
| Bond angles, ° | 1.7 |
| Dihedral angles, ° | 21.5 |

*Values in parentheses are for the highest-resolution shell.
†$R_{sym} = \Sigma_h \Sigma_i |I_i(h) - \langle I(h)\rangle| / \Sigma_h \Sigma_i I_i(h)$, where $I_i(h)$ is the $i$th measurement.
‡The last shell $R_{sym}$ for the high-resolution set is rather high because of strong anisotropy.
§$R$ factor $= \Sigma_h ||F(h)_{obs}| - |F(h)_{calc}|| / \Sigma_h |F(h)_{obs}|$.
¶$R_{free}$ was calculated using ≈5% of the data, which was randomly selected and excluded from refinement.

ward-facing conformation(s). It follows that accessibility of the sugar-binding site to the outer surface of the membrane may represent the rate-limiting step in the transport mechanism.

Although affinity of LacY for ligand is essentially the same from both surfaces of the membrane (ref. 37; SI Fig. 4), a clear sugar density is not observed in the native structure of wild-type LacY, despite many attempts at crystallization with supersaturating concentrations of TDG. However, site-directed alkylation studies (6) indicate that ligand binding induces a conformation that is at a higher free-energy state than apo LacY. Isothermal calorimetry measurements (38) also indicate that there are multiple ligand-bound conformers in the wild type. Single-molecule FRET (7) and double-electron electron resonance (44) indicate further that ligand binding shifts the population of conformers to intermediate and outward-facing forms. Therefore, it is likely that the ligand-bound form of LacY may not be in the lowest free-energy state but in an intermediate conformation not observed in any of the crystal structures thus far.

The C154G mutant binds ligand from either side of the membrane with similar affinities that are comparable to the wild type (SI Fig. 4), but sugar translocation across the membrane is essentially nil in either direction (SI Fig. 5*B*) (4, 5, 11). With *p*-nitrophenyl α-D-galactopyranoside binding to the C154G mutant, a large negative change in enthalpy and a decrease in entropy are observed, suggesting there are fewer conformers in the ligand-bound form relative to wild-type LacY (38). Single-molecule FRET (7) and double-electron electron resonance (6, 45) studies indicate that ligand induces closing of the inward-facing cavity with little or no change on periplasmic side of C154G. Therefore, it is likely that ligand binding from either side of C154G causes the protein to assume a ligand-bound intermediate conformation(s) that is unable to further undergo the global conformational change essential for turnover.

Because all of the x-ray structures of LacY are in the same conformation, it is likely that the crystallization process selects a single conformer of LacY that is in the lowest free-energy state.

## Materials and Methods

**Materials.** [1-$^{14}$C]Lactose was obtained from Amersham Pharmacia Biotechnology (Piscataway, NJ). *p*-Nitrophenyl α-D-[6-$^{3}$H]galactopyranoside was the generous gift of Gérard Leblanc (Université Pierre et Marie Curie, Observatoire Oceanologique, Villefranche-sur-Mer, France). Dodecyl β-D-maltopyranoside (DDM) was purchased from Anatrace (Maumee, OH). *E. coli* PL polar extract (catalog no. 100600) was obtained from Avanti (Alabaster, AL). Crystallization solutions and plates were purchased from Hampton Research (Aliso Viejo, CA). All other materials were reagent grade and obtained from commercial sources.

**Vector Construction, Protein Expression, and Purification.** Vector pT7–5/WT-LacY/C(His)$_{10}$ encoding wild-type LacY with a 10-His tag at the C terminus was constructed as described (12). Overexpression in *E. coli* XL1 Blue {*recA1 endA1 gyrA96 thi-1 hsdR17 supE44 relA1 lac* [F′ *proAB lacI*q*Z*Δ*M15* Tn*10* (Tetr)]}, membrane preparation, and protein purification by metal-affinity chromatography were carried out as described (2, 12). Immidazole eluates from the cobalt column (BD TALON Superflow resin) were dialyzed overnight against 5 liters of 20 mM Tris·HCl/0.01% DDM at a final pH of 7.5 (measured on ice) and concentrated with a Vivapspin concentrator by using a 50-kDa molecular mass cutoff.

**PL Preparation.** *E. coli* PL polar extract was solubilized in 0.5% DDM at a concentration of ≈30 mM, gassed with argon, and stored at −80°C until use. PL was added to the purified protein at final concentrations from 0 to 1.5 mM before crystallization.

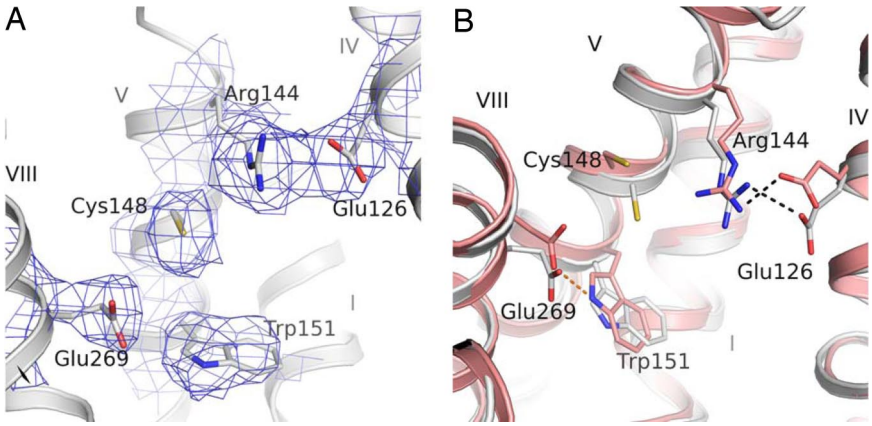


**Fig. 2.** Substrate-binding site. (*A*) $2F_o - F_c$ electron density (blue) contoured at 1 σ around residues (gray) located in the sugar-binding site. (*B*) Superposition of sugar-binding residues from wild-type (gray) and C154G LacY (pink; 2cfq). Salt bridges (Arg-144/Glu-126) are shown as black dotted lines, and an H bond (Glu-269–Trp-151) in C154G is shown as a pink dotted line.

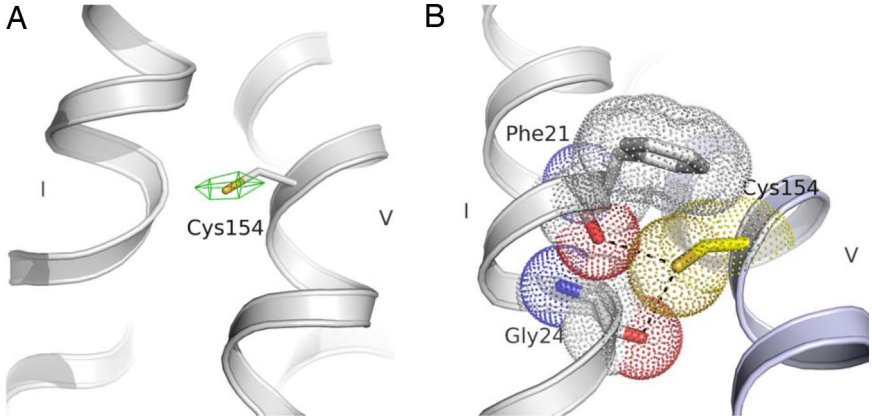


**Fig. 3.** Cys-154. (*A*) $F_o - F_c$ electron density map (green) contoured at 4 $\sigma$ around residue Cys-154. The map was calculated during refinement before residue 154 was changed to Cys from Gly. The map pinpoints the position of the Cys-154 sulfur. (*B*) The side chains of Cys-154 (yellow, helix V), Phe-21/Gly-24 (gray, helix I), and backbone carbonyl oxygen (red), as well as nitrogen (blue), are shown as sticks surrounded by van der Waals dots. The H bonds are shown as broken dots.

**Crystallization.** All protein samples were centrifuged at 327,205 × *g* for 1 h in a TLA100.1 rotor to remove aggregates. Crystallization was then carried out in the presence of 5 mM TDG by hanging drop vapor diffusion. Briefly, a 1-$\mu$l protein solution was mixed with 1 $\mu$l of a freshly prepared solution consisting of 8 $\mu$l of reservoir [0.1 M Hepes (pH 8.0)/0.1 M ammonium sulfate/29–31% PEG 400], 1 $\mu$l of 80 mM CHAPS and 1 $\mu$l of 30% 1,6-hexanediol. The 2-$\mu$l drops were equilibrated against 300 $\mu$l of reservoir solution at 23°C, and crystals were grown within 3–4 days.

**Diffraction and Data Collection.** Crystals of wild-type LacY were screened by direct freezing in liquid nitrogen and x-ray diffraction at 100 K with a synchrotron source at one of the following beamlines: BL 8.2.1 at the Advanced Light Source (ALS) at Lawrence Berkeley National Laboratory (Berkeley, CA) or X06SA at the Swiss Light Source (Villigen, Switzerland). The data set was collected at BL 8.2.1 at ALS. The software strategy in the HKL 2000 package was used to guide data collection. Diffraction data were processed by using Denzo and Scalepack (39). The crystal diffracted to 3.6 Å in one and 4.5 Å in the other dimension, respectively, and belongs to the orthorhombic space group $P2_12_12_1$. Data statistics are summarized in Table 1.

**Structure Determination and Refinement.** The structure was solved by using isomorphous molecular replacement using the 1PV7 structure (2). Subsequent refinement of the structure was carried out by using CNS (40) initially with rigid body minimization with the entire molecule and then three separate rigid bodies [residues 1–190 (N-terminal six-helix bundle), 191–210 (central loop between helix VI and VII), and 211–417 (C-terminal six-helix bundle)] followed by simulated annealing, individual restrained B-factor refinement, and minimization. CNS constraints were used throughout the refinement; in the last two rounds, strict restraints were used. Approximately 5% of the data was set aside for calculation of $R_{free}$ values. Manual rebuilding was done by using O (41) with sigma A-weighted $2F_o - F_c$ and $F_o - F_c$ electron density maps (42). The stereochemistry of the model was evaluated by using Procheck (43). All refinement statistics are given in Table 1. None of the residues were found in the disallowed, 4.1% in the generously allowed, 35.3% in the additionally allowed, and 60.6% in the most favored regions. The electron densities throughout the structure were clear, and most of the aminoacyl side chains were easily assigned, with the exceptions of the central cytoplasmic loop (residues 191–205) and the C-terminal helix (residues 404–417) where some of the side chains exhibited poor density.

We are indebted to the BL 8.2.1 at the Advanced Light Source at Lawrence Berkeley National Laboratory and the X06SA at the Swiss Light Source for use of synchrotrons. We thank Mariae Choi for technical support. This work was supported in part by National Institutes of Health Grants DK51131 and DK06946 and by National Science Foundation Grant 0450970 (to H.R.K.) and in part by Biotechnology and Biological Sciences Research Council grants (S.I.). In particular, work with PL was supported in part by National Institutes of Health Grants 1 P50 GM073210 and 1 U54 GM074929 (to H.R.K.).

1. Guan L, Kaback HR (2006) *Annu Rev Biophys Biomol Struct* 35:67–91.
2. Abramson J, Smirnova I, Kasho V, Verner G, Kaback HR, Iwata S (2003) *Science* 301:610–615.
3. Mirza O, Guan L, Verner G, Iwata S, Kaback HR (2006) *EMBO J* 25:1177–1183.
4. Menick DR, Sarkar HK, Poonian MS, Kaback HR (1985) *Biochem Biophys Res Commun* 132:162–170.
5. Smirnova IN, Kaback HR (2003) *Biochemistry* 42:3025–3031.
6. Kaback HR, Dunten R, Frillingos S, Venkatesan P, Kwaw I, Zhang W, Ermolova N (2007) *Proc Natl Acad Sci USA* 104:491–494.
7. Majumdar DS, Smirnova I, Kasho V, Nir E, Kong X, Weiss S, Kaback HR (2007) *Proc Natl Acad Sci USA* 104:12640–12645.
8. Huang Y, Lemieux MJ, Song J, Auer M, Wang DN (2003) *Science* 301:616–620.
9. Dawson RJ, Locher KP (2006) *Nature* 443:180–185.
10. Pinkett HW, Lee AT, Lum P, Locher KP, Rees DC (2007) *Science* 315:373–377.
11. Ermolova NV, Smirnova IN, Kasho VN, Kaback HR (2005) *Biochemistry* 44:7669–7677.
12. Guan L, Smirnova IN, Verner G, Nagamoni S, Kaback HR (2006) *Proc Natl Acad Sci USA* 103:1723–1726.
13. Yin Y, He X, Szewczyk P, Nguyen T, Chang G (2006) *Science* 312:741–744.
14. Pao SS, Paulsen IT, Saier MH, Jr (1998) *Microbiol Mol Biol Rev* 62:1–32.
15. Guan L, Murphy FD, Kaback HR (2002) *Proc Natl Acad Sci USA* 99:3475–3480.
16. le Coutre J, Kaback HR, Patel CK, Heginbotham L, Miller C (1998) *Proc Natl Acad Sci USA* 95:6114–6117.
17. Patzlaff JS, Moeller JA, Barry BA, Brooker RJ (1998) *Biochemistry* 37:15363–15375.
18. Frillingos S, Gonzalez A, Kaback HR (1997) *Biochemistry* 36:14284–14290.
19. Sahin-Tóth M, le Coutre J, Kharabi D, le Maire G, Lee JC, Kaback HR (1999) *Biochemistry* 38:813–819.
20. Wolin CD, Kaback HR (2000) *Biochemistry* 39:6130–6135.
21. Weinglass AB, Whitelegge JP, Hu Y, Verner GE, Faull KF, Kaback HR (2003) *EMBO J* 22:1467–1477.
22. Vazquez-Ibar JL, Guan L, Weinglass AB, Verner G, Gordillo R, Kaback HR (2004) *J Biol Chem* 279:49214–49221.
23. Jung H, Jung K, Kaback HR (1994) *Biochemistry* 33:12160–12165.
24. Wu J, Kaback HR (1994) *Biochemistry* 33:12166–12171.
25. Frillingos S, Kaback HR (1996) *Biochemistry* 35:3950–3956.
26. le Coutre J, Kaback HK (2000) *Biopolymers* 55:297–307.

27. Guan L, Sahin-Tóth M, Kaback HR (2002) *Proc Natl Acad Sci USA* 99:6613–6618.
28. Guan L, Hu Y, Kaback HR (2003) *Biochemistry* 42:1377–1382.
29. Kaback HR, Sahin-Toth M, Weinglass AB (2001) *Nat Rev Mol Cell Biol* 2:610–620.
30. Palsdottir H, Hunte C (2004) *Biochim Biophys Acta* 1666:2–18.
31. Ostermeier C, Michel H (1997) *Curr Opin Struct Biol* 7:697–701.
32. Zhang H, Kurisu G, Smith JL, Cramer WA (2003) *Proc Natl Acad Sci USA* 100:5160–5163.
33. Jidenko M, Nielsen RC, Sorensen TL, Moller JV, le Maire M, Nissen P, Jaxel C (2005) *Proc Natl Acad Sci USA* 102:11687–11691.
34. Lemieux MJ, Song J, Kim MJ, Huang Y, Villa A, Auer M, Li XD, Wang DN (2003) *Protein Sci* 12:2748–2756.
35. Long SB, Campbell EB, Mackinnon R (2005) *Science* 309:897–903.
36. Guan L, Sahin-Toth M, Kalai T, Hideg K, Kaback HR (2003) *J Biol Chem* 278:10641–10648.
37. Guan L, Kaback HR (2004) *Proc Natl Acad Sci USA* 101:12148–12152.
38. Nie Y, Smirnova I, Kasho V, Kaback HR (2006) *J Biol Chem* 281:35779–35784.
39. Otwinowski Z, Minor W (1997) in *Methods in Enzymology* (Academic, New York), Vol 276, pp 307–326.
40. Brünger A, Adams P, Clore G, DeLano W, Gros P, Grosse-Kunstleve R, Jiang J, Kuszewski J, Nilges M, Pannu N, *et al.* (1998) *Acta Crystallogr* D54:905–921.
41. Jones T, Kennedy E (1969) *J Biol Chem* 244:5981–5987.
42. Read R (1986) *Acta Crystallogr* A42:140–149.
43. Laskowski R, Rullmannn J, MacArthur M, Kaptein R, Thornton J (1996) *J Biomol NMR* 8:477–486.
44. Smirnova I, Kasho V, Choie J-Y, Altenbach C, Hubbell WL, Kaback HR (2007) *Proc Natl Acad Sci USA,* in press.
45. Nie Y, Ermolova N, Kaback HR (2007) *Proc Natl Acad Sci USA*, in press.